Published for SISSA by Springer

Received: June 17, 2014
Revised: November 12, 2014
Accepted: November 12, 2014
Published: December 4, 2014

Exotic Higgs decays in the golden channel

Adam Falkowski and Roberto Vega-Morales

Laboratoire de Physique Théorique, CNRS-UMR 8627, Université de Paris-Sud 11, F-91405 Orsay Cedex, France

E-mail: adam.falkowski@th.u-psud.fr, rvegamorales@gmail.com

Abstract: The Higgs boson may have decay channels that are not predicted by the Standard Model. We discuss the prospects of probing exotic Higgs decays at the LHC using the 4-lepton final state. We study two specific scenarios, with new particles appearing in the intermediate state of the $h \to 4\ell$ decay. In one, Higgs decays to a Z boson and a new massive gauge boson, the so-called hidden photon. In the other, Higgs decays to an electron or a muon and a new vector-like fermion. We argue that the upcoming LHC run will be able to explore a new parameter space of these models that is allowed by current precision constraints. Employing matrix element methods, we use the full information contained in the differential distribution of the 4-lepton final state to extract the signal of exotic decays. We find that, in some cases, the LHC can be sensitive to new physics even when the correction to the total $h \to 4\ell$ rate is of the order of a percent. In particular, for the simplest realization of the hidden photon with the mass between 15 and 65 GeV, new parameter space can be explored in the LHC run-II.

Keywords: Higgs Physics, Beyond Standard Model

ArXiv ePrint: 1405.1095

doi:10.1007/JHEP12(2014)037

JHEP12(2014)037

Contents

JHEP12(2014)037

1 Introduction

The particle with mass $m_h \approx 125.6\,\text{GeV}$ discovered at the LHC is so far perfectly compatible with being the Standard Model (SM) Higgs boson [1, 2]. It is nevertheless conceivable that more in-depth studies will reveal its non-standard properties. In particular, the Higgs may have exotic decay channels, that is channels not predicted in the SM or predicted to occur with a negligible branching fraction. Many scenarios beyond the SM predict new Higgs decay channels, especially in the presence of new degrees of freedom with $m \lesssim m_h$. The existing LHC searches for exotic Higgs decays cover decays to invisible particles [3, 4], to 4 photons [5] or 4 muons via new [6, 7] intermediate bosons, to electron jets [8], and to long-lived neutral particles [9, 10]. However many more interesting final states and topologies exist [11–16]; see ref. [16] for a comprehensive review. It should be noted that the current Higgs data can easily accommodate an order 20% branching fraction for exotic decays, and even more if the Higgs production cross section is enhanced, and/or Higgs couplings to the SM matter are modified, see figure 1. Furthermore, the sizable Higgs production cross section at the LHC allows us to probe much smaller branching fractions: down to $\sim 10^{-5}$ currently, and down to $\sim 10^{-9}$ in the future 100 TeV collider, as long as the final state is experimentally clean. All this makes exotic Higgs decays an attractive direction to search for new physics.

One very promising [13, 16] signature for this kind of searches is the so-called *golden channel*: the 4ℓ final state, $\ell = e, \mu$, with two opposite-sign same-flavor lepton pairs. Thanks to the fully reconstructible kinematics, low background, and small systematic errors it was one of the early Higgs discovery channels despite the small branching fraction. At the same time, order one new physics corrections to the SM rate in this channel can be accommodated at this point. Assuming the Higgs production cross section is unchanged

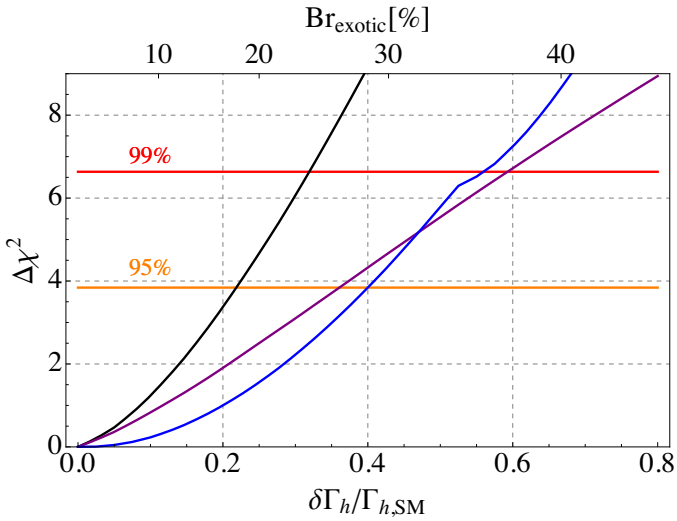

Figure 1. Global fit to the Higgs data in the presence of an exotic contribution to the Higgs decay width $\delta\Gamma_h$. The black curve assumes the Higgs production cross section and relative branching fraction to the SM matter are fixed at the SM values, which leads to the indirect limit $\mathrm{Br}(h \to \text{exotic}) \lesssim 18\%$ at 95% CL. This limit takes into account the uncertainty on the SM prediction of the gluon-fusion production cross-section which we take as 14.7% [19]. Leaving as a free parameter in the fit the gluon fusion production cross section (purple curve), and/or the Higgs branching fraction to b-quarks (blue curve), the limit is relaxed to $\mathrm{Br}(h \to \text{exotic}) \lesssim 30\%$. If all effective Higgs couplings to the SM are left free then only the model independent bound $\mathrm{Br}(h \to \text{exotic}) \lesssim 80\%$ applies, based on the direct Higgs width measurement in CMS [20].

from the SM, the event rates reported in refs. [17, 18] yield the 95% CL limits on the additional partial decay widths:

$$\frac{\Delta\Gamma_{h\to 4\mu}}{\Gamma^{\rm SM}_{h\to 4\mu}} < 0.90\,, \qquad \frac{\Delta\Gamma_{h\to 2e2\mu}}{\Gamma^{\rm SM}_{h\to 2e2\mu}} < 0.83\,, \qquad \frac{\Delta\Gamma_{h\to 4e}}{\Gamma^{\rm SM}_{h\to 4e}} < 1.27\,. \tag{1.1}$$

For new physics contributing to all sub-channels the limit is

$$\frac{\Delta\Gamma_{h\to 4\ell}}{\Gamma^{\rm SM}_{h\to 4\ell}} < 0.52\,. \tag{1.2}$$

Strictly speaking, the widths in eq. (1.1) and eq. (1.2) should be weighted by the efficiency to experimental cuts, which may differ in the presence new physics.

Apart from the event rate, the 4ℓ final state offers far more information in the form of the differential distribution in the decay angles and lepton pair invariant masses. In this paper we investigate the possibility of using this information to further constrain exotic decays of the Higgs boson. We employ the matrix element methods originally developed for the purpose of determining the structure of the Higgs couplings to the SM gauge bosons [21–23]. The starting point for our analysis is an analytic expression for the fully differential $h \to 4\ell$ matrix element, with and without the new physics contribution. Using this matrix element, we construct a likelihood function for a data set containing a number N of 4-lepton events. This likelihood function is then used to estimate the statistical significance for discrimination between the SM and exotic decays hypotheses as a function of N.

JHEP12(2014)037

We study two simple models that can accommodate sizable exotic branching fractions in the golden channel without violating current experimental constraints. The first one contains a new light gauge boson X coupled to the SM via the hypercharge portal $\epsilon X_{\mu\nu} B_{\mu\nu}$ [24]. The kinetic mixing induces the coupling of X to the electromagnetic current, and also the mixing between the Z boson and X. As a result, the Higgs boson can decay as $h \to XZ$ when it is kinematically allowed. When both X and Z decay leptonically, this new Higgs decay mode contributes to the 4ℓ final state. Another model we study here contains a new heavy vector-like charged lepton E transforming as $(1,1)_{-1}$ under the SM gauge group. After electroweak symmetry breaking E mixes with one of the SM leptons via Yukawa couplings. As a result, one obtains non-diagonal couplings to the Z and Higgs boson of the form $Z_\mu \bar{E}_L \gamma_\mu \ell_L + \text{h.c.}$ and $h \bar{E}_R \ell_L h + \text{h.c.}$. These couplings mediate the $h \to E\ell \to Z\ell\ell$ cascade decay that, for leptonic Z decays, again contributes to the 4-lepton final state.

The paper is organized as follows. In section 2 we describe our models in more detail. In section 3 we review the matrix element methods to extract information from the golden channel. Our results regarding the sensitivity of the golden channel to exotic Higgs decays are contained in section 4.

2 Models

In this section we study two scenarios where new light degrees of freedom can modify Higgs decays in the golden channel. One has a new light vector field (the hidden photon) kinetically mixing with the SM hypercharge. The other has a new vector-like fermion with quantum numbers of the SM right-handed electron that mixes via a Yukawa coupling with one of the SM charged leptons. We determine the region of the parameter space of these models allowed by precision measurements, and we discuss the limits on the branching fraction for exotic Higgs decays imposed by these constraints.

2.1 Hidden photon

The first model we study has cascade decay $h \to ZX \to 4\ell$ mediated by a new neutral vector boson. Consider a massive abelian gauge field X_μ interacting with the SM only via the hypercharge portal:

$$\mathcal{L} = \mathcal{L}_{\text{SM}} - \frac{1 - \epsilon^2 \cos^{-2}\theta_W}{4} \hat{X}_{\mu\nu} \hat{X}_{\mu\nu} + \frac{1}{2} \hat{m}_X^2 \hat{X}_\mu \hat{X}_\mu + \frac{\epsilon}{2\cos\theta_W} B_{\mu\nu} \hat{X}_{\mu\nu} \,. \tag{2.1}$$

Here θ_W is the Weinberg angle, and the non-standard normalization of the X kinetic term is introduced for future convenience. We assume $\epsilon \ll 1$ and determine the spectrum and couplings perturbatively in ϵ. The mass term $\hat{m}_X$ could be generated via the Stückelberg mechanism, or via an expectation value of a hidden sector Higgs field; in the latter case we will assume the corresponding hidden Higgs boson is heavy enough such that it does not affect the hidden photon decays. We are interested in $\hat{m}_X \ll m_Z$, such that X can have a non-negligible effect on Higgs decays.

JHEP12(2014)037

To work out the model's phenomenology it is convenient to remove the kinetic mixing by redefining the hypercharge gauge field: $B_\mu \to B_\mu + \cos\theta_W^{-1}\hat{X}_\mu$. The kinetic terms are now diagonal and canonically normalized, but after the EW breaking the Z and X bosons mix via the mass terms,

$$\mathcal{L}_{\rm mass} = \frac{1}{2}\hat{m}_Z^2\hat{Z}_\mu\hat{Z}_\mu + \frac{1}{2}(\hat{m}_X^2 + \epsilon^2\hat{m}_Z^2\tan^2\theta_W)\hat{X}_\mu\hat{X}_\mu - \hat{m}_Z^2\epsilon\tan\theta_W\hat{X}_\mu\hat{Z}_\mu\,, \tag{2.2}$$

where $\hat{m}_Z = \sqrt{g_L^2+g_Y^2}v/2$ and we denote g_L, g_Y the SM gauge couplings of $\mathrm{SU}(2)_L\times\mathrm{U}(1)_Y$. To diagonalize the mass matrix we need the rotation

$$\hat{Z}_\mu = \cos\alpha Z_\mu + \sin\alpha X_\mu\,, \qquad \hat{X}_\mu = -\sin\alpha Z_\mu + \cos\alpha X_\mu\,, \qquad \alpha \approx \epsilon\tan\theta_W\frac{m_Z^2}{m_Z^2-m_X^2} + \mathcal{O}(\epsilon^2)\,. \tag{2.3}$$

Mixing between the Z and exotic bosons is constrained electroweak precision observables. In particular, it affects the mass of the Z boson,

$$m_Z^2 = \hat{m}_Z^2 + \epsilon^2\frac{\tan^2\theta_W\hat{m}_Z^4}{m_Z^2-\hat{m}_X^2} + \mathcal{O}(\epsilon^3)\,, \tag{2.4}$$

and the Z boson couplings to matter,

$$g_{Z,f} = \hat{g}_{Z,f}\left(1-\epsilon^2\frac{\tan^2\theta_W m_Z^4}{(m_Z^2-m_X^2)^2}\right) - \epsilon^2\sqrt{g_L^2+g_Y^2}\frac{\tan^2\theta_W m_Z^2}{m_Z^2-m_X^2}Y_f\,, \tag{2.5}$$

where $\hat{g}_{Z,f} = \sqrt{g_L^2+g_Y^2}(T_f^3 - \sin^2\theta_W Q_f)$ is the Z boson coupling in the SM. Using the constraints from LEP-1 and SLC [25] and W mass [26] measurements for $m_X \ll m_Z$ we find

$$|\epsilon| \lesssim 0.024\sqrt{1-\frac{m_X^2}{m_Z^2}} \qquad \text{at } 95\%\,\mathrm{CL}\,, \tag{2.6}$$

in agreement with ref. [27]. For m_X below 9.3 GeV one gets a stronger limit $|\epsilon| \lesssim 10^{-3}$ [16, 28] based on $\Upsilon(2S,3S) \to \gamma\mu^+\mu^-$ searches in BaBar [29].

We turn to the couplings of the hidden photon. The couplings to the SM fermion are

$$g_{X,f} = \epsilon\, e\left[Q_f\left(1-\frac{\tan^2\theta_W m_X^2}{m_Z^2-m_X^2}\right) + T_f^3\frac{m_X^2}{\cos^2\theta_W(m_Z^2-m_X^2)}\right]. \tag{2.7}$$

The new vector field couples to the electromagnetic current up to $\mathcal{O}(m_X^2/m_Z^2)$ corrections, hence the name *hidden photon*. Assuming there's no other decay channels of X (in particular, there is no decay to other particles in the hidden sector), for $m_X \ll m_Z$ one finds $\mathrm{Br}(X\to l^+l^-)\approx 0.15$, $\mathrm{Br}(X\to \mathrm{had})\approx 0.55$, while $\mathrm{Br}(X\to\nu\nu)$ is negligible. Due to the mixing with Z, the hidden photon also acquires the coupling to the Higgs boson:

$$\mathcal{L}_{hZX} = c_{hZX}\frac{m_Z^2}{v}hZ_\mu X_\mu\,, \qquad c_{hZX} = \frac{2\epsilon\tan\theta_W m_X^2}{m_Z^2-m_X^2} + \mathcal{O}(\epsilon^2)\,. \tag{2.8}$$

Thus, all elements are in place for new contributions to the golden channel via the cascade decay $h\to ZX\to 4\ell$. However, the coupling in eq. (2.8) is suppressed not only by ϵ but

JHEP12(2014)037

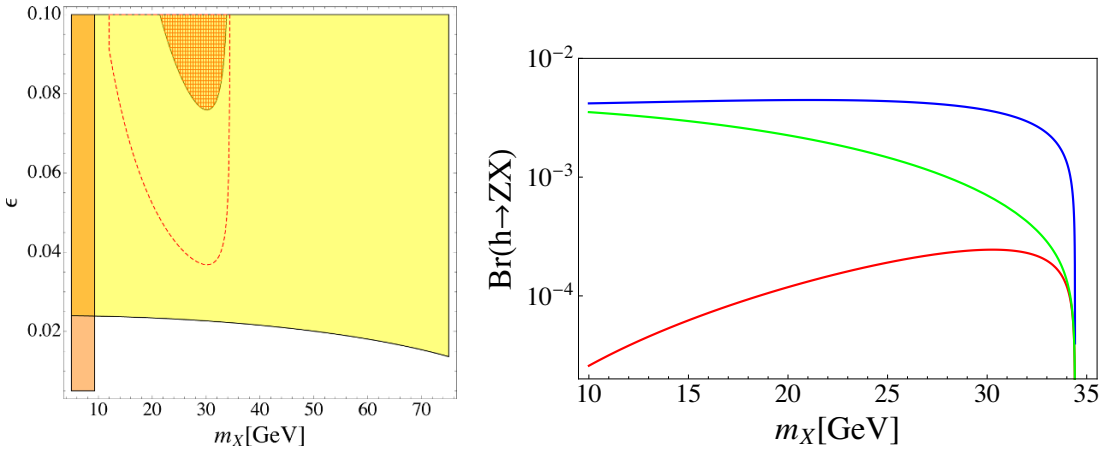

Figure 2. *Left*: the parameter space in the mass vs. mixing plane for a hidden photon mixing with the SM hypercharge gauge boson. For this plot we assume $\epsilon_2 = \epsilon_3 = 0$. The yellow and orange areas are excluded respectively by direct BaBar searches and by electroweak precision constraints. The red mesh area is excluded by the observed $h \to 4\ell$ event rate, taking into account $h \to XZ$ decays with both X and Z on-shell, and assuming the Higgs couplings to the SM matter are not modified). The red dashed line shows an estimated expected limit based on the 4-lepton event rate information with 300 fb^{-1} at 14 TeV LHC. *Right*: the branching fraction for $h \to XZ$ in the hidden photon model for $\epsilon = 0.02$ and $\epsilon_2 = \epsilon_3 = 0$ (red), $\epsilon_2 = 0.02$, $\epsilon_3 = 0$ (blue), and $\epsilon_2 = 0$, $\epsilon_3 = 0.02$ (green).

also by m_X^2/m_Z^2. For this reason, the maximum $\mathrm{Br}(h \to ZX)$ does not exceed 2.5×10^{-4}, as can be read off from the right panel of figure 2. Currently, such a small branching fraction is not constrained by the observed $h \to 4\ell$ event rate. Even scaling the present sensitivity to 300 fb^{-1} of data at 14 TeV LHC, the rate information alone does not allow one to explore the parameter space that is not excluded by precision measurements, see the left panel of figure 2. Somewhat stronger limits can be obtained when the input from the dilepton invariant mass distribution is used [16], but these limits are still weaker than the ones from electroweak precision tests. In section 4 we will argue that the sensitivity can be further enhanced by using the full information contained in the differential distribution of $h \to 4\ell$ decays.

A larger 4-lepton branching fraction can be obtained by modifying the model. One way is to introduce mixing between the SM and the hidden Higgs boson S that subsequently decays as $S \to XX$ [30]. Here we consider another simple modification. One can introduce additional couplings between the hidden photon and the SM sector [31]:

$$\Delta\mathcal{L} = \frac{\epsilon_2}{\cos\theta_W}\left(\frac{|H|^2}{v^2} - \frac{1}{2}\right) B_{\mu\nu}\hat{X}_{\mu\nu} + \frac{\epsilon_3}{\cos\theta_W}\frac{|H|^2}{v^2}\tilde{B}_{\mu\nu}\hat{X}_{\mu\nu}\,, \tag{2.9}$$

where $\tilde{B}_{\mu\nu} = \epsilon_{\mu\nu\rho\sigma}\partial_\rho B_\sigma$. The new terms in $\Delta\mathcal{L}$ induce new couplings of the Higgs boson to the Z boson and the hidden photon:

$$\Delta\mathcal{L}_{hXZ} = -\frac{h}{v}\tan\theta_W(\epsilon_2 X_{\mu\nu}Z_{\mu\nu} + \epsilon_3 X_{\mu\nu}\tilde{Z}_{\mu\nu}) + \mathcal{O}(\epsilon^2)\,. \tag{2.10}$$

JHEP12(2014)037

In principle, the parameters ϵ_2 and ϵ_3 are not constrained by precision observables (although $|\epsilon_2| \gg |\epsilon|$ would be fine-tuning).[1] Furthermore, the Higgs couplings in eq. (2.10) are not suppressed by m_X^2/m_Z^2, unlike in the vanilla model. For these reasons, this deformation of the hidden photon model allows for a sizable branching fraction for $h \to XZ$ decay. In fact, the strongest constraints on ϵ_2 and ϵ_3 currently come from the $h \to 4\ell$ searches.

We note that for $\epsilon_{2,3} \neq 0$ the model also contains the $hX\gamma$ couplings:

$$\Delta\mathcal{L}_{hX\gamma} = \frac{h}{v}(\epsilon_2 X_{\mu\nu} A_{\mu\nu} + \epsilon_3 X_{\mu\nu} \tilde{A}_{\mu\nu}) + \mathcal{O}(\epsilon^2)\,. \tag{2.11}$$

It leads to an additional contribution to the $h \to 4\ell$ decay, with an off-shell photon instead of Z. The size of this contribution strongly depends on the experimental cuts on the final state leptons.[2] We find that for the standard CMS cuts the photon mediated contribution affects the new physics corrections to the 4ℓ event rate by an $\mathcal{O}(1)$ factor. Another consequence of the couplings in eq. (2.11) is the presence of $h \to X\gamma$ decays with an off-shell photon. The branching fraction is larger than that for $h \to XZ$ decays because the $hX\gamma$ coupling is larger by $\tan^{-1}\theta_W$, and because there is less phase space suppression. For example, for $\epsilon_2 = 0.02$ or $\epsilon_3 = 0.02$ one finds $\mathrm{Br}(h \to X\gamma) \approx 10\%$. Therefore this version of the hidden photon model can also be probed in the $h \to \ell^+\ell^-\gamma$ final state. We postpone to a future publication quantitative studies of the sensitivity of the $h \to \ell^+\ell^-\gamma$ channel to exotic Higgs decays.

2.2 Vector-like lepton

The other scenario we study in this paper is the one where Higgs decays can proceed as $h \to El \to Z\ell^+\ell^- \to 4\ell$, mediated by a new charged lepton mixing with the SM leptons. Consider the SM extended by a vector-like fermion E transforming under the SM gauge group as $(1,1)_{-1}$, thus having quantum numbers of the right-handed electron. We assume E mixes with one of the SM charged leptons via Yukawa couplings. The part of the Lagrangian giving rise to the vector-like and SM lepton masses is given by

$$\mathcal{L} = -y\bar{\ell}_R H^\dagger l_L - M_E \bar{E}_R E_L - Y \bar{E}_R H^\dagger l + \text{h.c.}\,, \tag{2.12}$$

where $l_L = (\nu_L, \ell_L)$, and ℓ could be electron, muon, or tau. The first term is the usual SM lepton Yukawa coupling. The second is a vector-like mass M_E of the heavy fermion. The last term leads to a mixing between the vector-like and the SM lepton after electroweak symmetry breaking. We assume $Yv \ll M_E$ and $yv \ll M_E$, in which case the lepton mass eigenstates of the mass matrix can be worked out perturbatively in v. To diagonalize the mass matrix we make the rotation

$$\begin{aligned} \ell_L &\to \cos\alpha_L \ell_L + \sin\alpha_L E_L\,, & E_L &\to -\sin\alpha_L \ell_L + \cos\alpha_L E_L\,, \\ \ell_R &\to \cos\alpha_R \ell_R + \sin\alpha_R E_R\,, & E_R &\to -\sin\alpha_R \ell_R + \cos\alpha_R E_R\,, \end{aligned} \tag{2.13}$$

[1] Note that the CP-odd kinetic mixing term $\tilde{B}_{\mu\nu}\hat{X}_{\mu\nu}$ is a total derivative and has no physical consequences.

[2] The inclusive $h \to 4l$ rate is IR divergent at the tree-level when diagrams with an intermediate photon are included.

JHEP12(2014)037

where the mixing angles are

$$\alpha_L = \frac{Yv}{\sqrt{2}M_E}\left(1+\mathcal{O}(v^2/M_E^2)\right), \qquad \alpha_R = \mathcal{O}(v^2/M_E^2)\,. \tag{2.14}$$

Thus, at the leading order, only left-handed charged leptons mix with the vector-like lepton. The mass of the heavy lepton is approximately M_E, and the mass of the SM lepton is approximately $yv/\sqrt{2}$, up to $\mathcal{O}(v^2/M_E^2)$ corrections.

Because E_L and ℓ_L have different quantum numbers under the EW group, the mixing affects the lepton couplings to W and Z. At the leading order one obtains non-diagonal lepton couplings to W and Z bosons,

$$\mathcal{L} = \frac{g_L}{\sqrt{2}}\alpha_L W^+_\mu \bar{\nu}_L\gamma_\mu E_L - \frac{\sqrt{g_L^2+g_Y^2}}{2}\alpha_L Z_\mu \bar{\ell}_L\gamma_\mu E_L \tag{2.15}$$

These couplings allow the heavy lepton to decay as $E \to Z\ell$ or as $E \to W\nu$, and we assume here that E has no other decay channels. For M_E close to m_Z the branching fractions strongly depend on M_E (due to the phase space suppression), and $\mathrm{Br}(E \to Z\ell)$ varies between 10% and 25% for M_E between 100 and 125 GeV. The Higgs boson also obtains non-diagonal couplings to the leptons:

$$\mathcal{L} = -\frac{Y}{\sqrt{2}}h\bar{E}_R\ell_L + \text{h.c.}\,. \tag{2.16}$$

At the end of the day, for $m_Z < M_E < m_h$, the Higgs boson can cascade decay as $h \to El \to Z\ell^+\ell^- \to 4\ell$.

The mass of the heavy lepton is constrained by direct LEP-2 searches $M_E \gtrsim 103\,\mathrm{GeV}$ [32]. So far the LHC experiments have not provided new limits on M_E, while a recast of generic multi-lepton searches [33] concluded that and SU(2) singlet E with M_E in the 100 GeV ballpark is not excluded [34]. Furthermore, the mixing angle α_L is constrained by electroweak precision tests. At the second-order in v the couplings of the SM left-handed charged leptons to W and Z are modified as

$$\mathcal{L} = \left(1-\frac{\alpha_L^2}{2}\right)\frac{g_L}{\sqrt{2}}W^+_\mu\bar{\nu}_L\gamma_\mu\ell_L + \left(\frac{-g_L^2+g_Y^2}{2\sqrt{g_L^2+g_Y^2}} + \sqrt{g_L^2+g_Y^2}\frac{\alpha_L^2}{2}\right)Z_\mu\bar{\ell}_L\gamma_\mu\ell_L\,. \tag{2.17}$$

The precise constraint on α_L somewhat depends on whether E mixes with e, μ, or τ. Using the electroweak precision measurements from LEP-1 and SLC [25] and the recent W mass measurements [26] we find the following 95% CL limits:

$$\begin{aligned} &(e) \qquad \alpha_L < 0.017\,,\\ &(\mu) \qquad \alpha_L < 0.030\,,\\ &(\tau) \qquad \alpha_L < 0.050\,. \end{aligned} \tag{2.18}$$

For a given M_E this translates into upper limits on the Yukawa coupling Y, and in consequence into upper limits on $\mathrm{Br}(h \to E\ell)$. The maximum allowed branching fractions in

JHEP12(2014)037

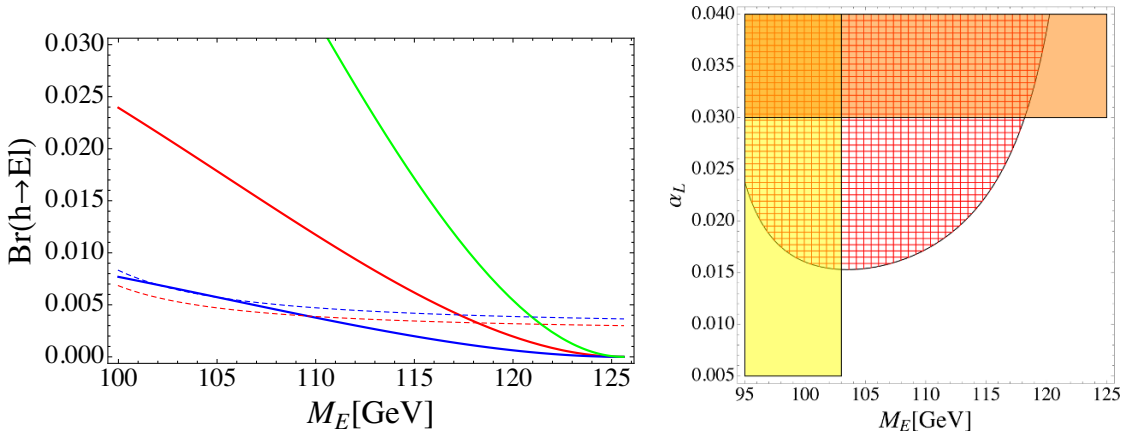

Figure 3. *Left*: the maximum branching fraction for $h \to E\ell$ decays allowed by electroweak precision constraints for $\ell = e$ (blue), $\ell = \mu$ (red), and $\ell = \tau$ (green), as a function of the E mass. The dashed lines indicate the current upper limits on $\mathrm{Br}(h \to E\ell)$ from the observed $h \to 4$ lepton event rate for $\ell = e$ (blue), and $\ell = \mu$ (red). *Right*: the allowed parameter space in the mass-mixing angle plane for a vector-like SU(2) singlet fermion E mixing with the SM muon. The yellow and orange areas are excluded respectively by direct LEP-2 searches and by electroweak precision constraints. The red mesh area is excluded by the observed $h \to 4\ell$ event rate (assuming the Higgs couplings to the SM are not modified).

the electron, muon and tau channels are shown in the left panel of figure 3. These limits turn out to be weak enough to allow an observable signal in the golden channel. In fact, the limits on additional width in the golden channel in eq. (1.1) already exclude a sizable chunk of otherwise viable parameter space. We conclude that vector-like leptons with mass $M_E \lesssim 125\,\mathrm{GeV}$ can be meaningfully probed by exotic Higgs decays.

3 Methods

We are interested in estimating the potential of LHC Higgs searches in the 4-lepton final state to constrain or discover exotic Higgs decays in the models described in section 2. To distinguish the SM $h \to ZZ^* \to 4\ell$ decays from those involving a new hidden photon or heavy fermion, we employ a simplified likelihood analysis following closely the procedure used in ref. [35] and described in more detail in [36, 37]. The $h \to 4\ell$ channel has a good signal-to-background ratio in the signal region $m_{4\ell} \approx m_h$, and is very well discriminated from the backgrounds due to the different shapes in the distributions of the various observables [38]. Of course, ideally one would include the dominant $q\bar{q} \to 4\ell$ background as well in the discriminator in order to make a precise statement about the sensitivity. However, recent studies [21, 22, 38] indicate that the effects of including the background should be small enough that for the present purposes considering the signal only is sufficient.

The starting point for our analysis is an analytic expression for the fully differential $h \to 2e2\mu$ decay width. In the models we consider the decay amplitude receive interfering contributions from the $h \to ZZ^* \to 2e2\mu$ diagram and from diagrams with an intermediate hidden photon or a vector-like charged fermion. We use it to build the probability density

JHEP12(2014)037

function (*pdf*)

$$\mathcal{P}_S(m_h^2, M_1, M_2, \vec{\Omega}|\vec{\lambda}) = \frac{d\Gamma_{h\to 4\ell}}{dM_1^2 dM_2^2 d\vec{\Omega}}\,. \tag{3.1}$$

Here M_1, M_2 are the invariant masses of the opposite-sign same-flavor lepton pairs, and the decay angles $\vec{\Omega} = (\Theta, \cos\theta_1, \cos\theta_2, \Phi_1, \Phi)$ are defined in [22]. The $\vec{\lambda}$ represent the parameters of the models to be considered. To compute the matrix element in the hidden photon model we modify the results of [38] to include the new gauge boson contribution. The matrix element in the vector-like lepton model is computed in the FeynArts/FormCalc framework [39] using a custom model exported from Feynrules [40]. In all cases the interference between the new physics process and the SM is included. Throughout we fix the Higgs boson mass as $m_h = 125.6\,\text{GeV}$.

With the *pdfs* at hand we can write the likelihood of obtaining a particular data set containing N events as,

$$L(\vec{\lambda}) = \prod_{\mathcal{O}}^{N} \mathcal{P}_S(\mathcal{O}|\vec{\lambda})\,, \tag{3.2}$$

where $\mathcal{O} = (m_h^2, M_1, M_2, \vec{\Omega})$. We then construct a simple hypothesis test [41] where as our test statistic we use the log likelihood ratio defined as,

$$\Lambda = 2\log\left[\mathcal{L}(\vec{\lambda}_1)/\mathcal{L}(\vec{\lambda}_2)\right]. \tag{3.3}$$

To estimate the expected significance of discriminating between two different hypotheses, we take one hypothesis as true, say $\vec{\lambda}_1$ and generate a set of N $\vec{\lambda}_1$ events. We then construct Λ for a large number of pseudo-experiments each containing N events in order to obtain a distribution for Λ. We repeat this exercise taking $\vec{\lambda}_2$ to be true and obtain a different distribution for Λ. With the two distributions for Λ in hand we can compute an approximate significance by denoting the distribution with negative mean as f and the distribution with positive mean as g and finding a value $\hat{\Lambda}$ such that

$$\int_{\hat{\Lambda}}^{\infty} f dx = \int_{-\infty}^{\hat{\Lambda}} g dx\,. \tag{3.4}$$

We then interpret this probability as a one sided Gaussian p-value, which can be used to compute the expected significance for discriminating between hypotheses (see [35] for more details). For a simple hypothesis test, this Gaussian approximation is often sufficient [41]. This procedure is repeated many times for a range of numbers of events N to obtain a significance as a function of N for each hypothesis. In our simplified framework we have also neglected any detector or production effects, but these effects are small and are not needed for the level of precision we aim for in this study [21, 22].

For the particular models considered here, $\vec{\lambda}$ corresponds to the mass of the new particle and the model parameters determining their coupling to the Higgs and leptons. Specifically, for the hidden photon model $\vec{\lambda} = (m_X, \epsilon, \epsilon_2, \epsilon_3)$, and for the vector-like lepton model $\vec{\lambda} = (M_E, Y)$. Our aim is to estimate whether the golden channel can probe the parameter space of these models that is not excluded by precision tests and direct searches. Various hypothesis tests to this end are conducted in the following section.

JHEP12(2014)037

4 Results

In this section we present our results concerning the sensitivity of the golden channel to exotic Higgs decays for the models described in section 2. To this end we pick a number of benchmarks point near the boundary of the parameter space region allowed by current constraints. We employ the matrix element approach described in section 3, where in our hypothesis tests we always compare our new physics model to the SM. For a given number N of events in the $h \to 2e2\mu$ channel we perform 1000–10000 pseudo-experiments to estimate the discriminating power between the SM and hidden photon mediated Higgs decays. We repeat this procedure over a range of N to obtain an estimate for the discriminating power as a function of number of events. For these pseudo-experiments we use the full available information contained in the differential distribution of the 4-lepton final state except for the total integrated event rate — we refer to this as *shape observables*. The motivation for separating the total rate is that it is less robust as a discriminator, as it can be affected by physics that has nothing to do with exotic decays, for example by modification of the effective Higgs coupling to gluons. We find that the discriminating power between the pure SM and hidden photon hypotheses comes mostly from M_1 and M_2 distributions, whereas angular variables add some discriminating power only in the extended hidden photon model of eq. (2.9). On the other hand, angular variables are important for separating the signal from the non-Higgs SM background. For a number of benchmark points we also show the results of combining the shape and the total rate observables. To reduce computing time, for large N we simply extrapolate our results obtained at lower N assuming the significance grows as $\sqrt{N}$. With these tools, we estimate the number of $h \to 2e2\mu$ events required to exclude our benchmark points at a given confidence level. Although we do not perform simulations in the $h \to 4\mu$ and $h \to 4e$ channels we expect that, after combining all 4-lepton channels, the sensitivity will correspond roughly to doubling the number of $h \to 2e2\mu$ events. To translate between the number of events and the LHC luminosity we assume the 27% efficiency of reconstructing 4-lepton Higgs decays (the one in CMS in the LHC run-I [18]). Thus, for example, $300\,\text{fb}^{-1}$ at 14 TeV LHC corresponds to roughly 275 $h \to 2e2\mu$ and 600 $h \to 4\ell$ expected events, where we take $\sigma(pp \to h) \approx 56\,\text{pb}$, and $\text{Br}(h \to 4\ell) = 1.3 \times 10^{-4}$ [19].

We start with the vanilla version of the hidden photon model that corresponds to setting $\epsilon_2 = \epsilon_3 = 0$ in eq. (2.9).[3] We fix $\epsilon = 10^{-2}$ for all benchmarks and consider several values of the hidden photon masses in the range 10–60 GeV. The benchmark points we studied are summarized in table 1 and our results concerning the LHC sensitivity are shown in figure 4. It is worth noting that for these points the total $h \to 4\ell$ rate is enhanced merely by a few percent compared to the SM. As this is within the uncertainty on the SM Higgs production cross section, the total rate information is not useful to discriminate between the SM and new physics in this case. Nevertheless, taking advantage of the full kinematic information contained in the 4-lepton event leads to a good sensitivity to new physics. We find that the parameter space of the hidden photon model allowed by electroweak precision observables can be probed already in the coming Run-II of the LHC.

[3] See refs. [30, 31, 43] for previous studies of the LHC sensitivity in this model.

JHEP12(2014)037

m_X	ϵ	ϵ_2	ϵ_3	R
10	0.02	0	0	1.004
15	0.02	0	0	1.006
20	0.02	0	0	1.019
25	0.02	0	0	1.031
30	0.02	0	0	1.039
30	0.02	0.01	0	1.33
30	0.02	0	0.015	1.20
35	0.02	0	0	1.019
40	0.02	0	0	1.019
50	0.02	0	0	1.016
60	0.018	0	0	1.014

m_E	α_L	R
103	0.015	1.48
110	0.017	1.57
115	0.02	1.08
120	0.02	0.95

Table 1. *Left*: benchmarks point for the hidden photon model. The 4-lepton event rate relative to the SM one $R = \frac{\Gamma(h\to 4\ell)}{\Gamma(h\to 4\ell)_{\rm SM}}$ was computed using MadGraph 5 [42] after imposing the standard CMS cuts: $p_{T,\ell} > 10\,\text{GeV}$, $|\eta_\ell| < 2.5$, and $M_1 > 50\,\text{GeV}$, $M_2 > 12\,\text{GeV}$ for opposite-sign, same-flavor lepton pairs. For the $m_X = 10\,\text{GeV}$ benchmark a weaker cut $M_2 > 5\,\text{GeV}$ is used, as the standard one cuts away most of the signal. For the benchmarks with non-zero ϵ_2 or ϵ_3 the rate includes the contribution of diagrams with an intermediate off-shell photon. *Right*: the same for the vector-like lepton mixing with the SM muon.

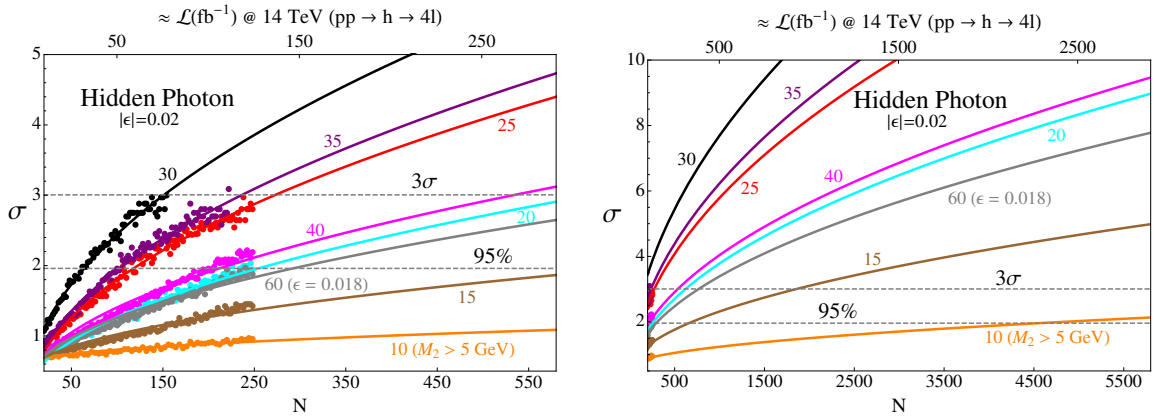

Figure 4. *Left*: the LHC sensitivity for the simplest version of the hidden photon model with $\epsilon_2 = \epsilon_3 = 0$ and $\epsilon = 10^{-2}$ for masses ranging from 10 to 60 GeV. The dots indicate the average σ obtain in our set of pseudo experiments which we have conducted for a range of fixed number of events from between $N = 20$ and $N = 600$. *Right*: same, extrapolated to larger N, assuming a $\sqrt{N}$ scaling in the sensitivity to estimate the discriminating power at high luminosity.

In particular, assuming $300\,\text{fb}^{-1}$ at 14 TeV will be collected, m_X in the range 15–65 GeV can be probed for ϵ near the boundary of the region allowed by precision observables. Further increase in sensitivity can be obtained in the high-luminosity phase of the LHC (assuming $3000\,\text{fb}^{-1}$ at 14 TeV) or in the future 100 TeV collider. In particular, the reach

JHEP12(2014)037

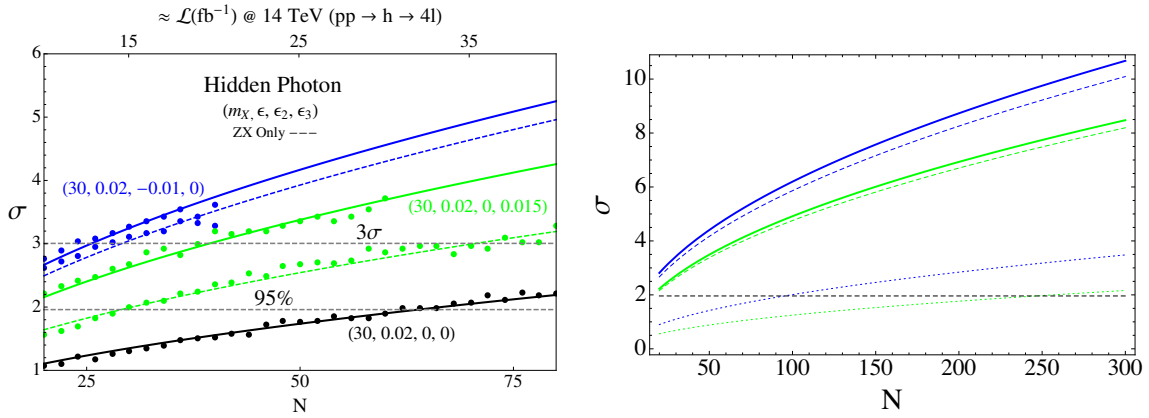

Figure 5. *Left*: lHC sensitivity using the shape of the 4-lepton distribution alone for the extended hidden photon points labeled by the values of $(m_X, \epsilon, \epsilon_2, \epsilon_3)$. The dots indicate the results obtained from conducting pseudo experiments which are then extrapolated to larger N assuming the significance grows as $\sqrt{N}$. The dashed curves indicate the sensitivity when only the hXZ couplings are taken into account; the difference between the dashed and solid curves demonstrates the importance of the off-shell photon contributions. *Right*: comparison of the discrimination power using the shape (dashed), rate (dotted), and combined shape+rate information (solid) for the extended hidden photon benchmarks with $m_X = 30\,\text{GeV}$, $\epsilon = 0.02$, and $(\epsilon_2, \epsilon_3) = (0.01, 0)$ (blue) and $(\epsilon_2, \epsilon_3) = (0, 0.015)$.

can be extended[4] down to $m_X = 10\,\text{GeV}$, below which the strong bounds on the kinetic mixing from B-factories make it difficult to probe the simplest hidden photon model in high-energy colliders. Note that the case with $m_X + m_Z > m_h$, where the strictly 2-body decay $h \to ZX$ is forbidden, can also be probed to some extent. In this case, the kinematic suppression due to the Z boson being strongly off-shell is partially offset by the fact that the hZX coupling increases with m_X. On the other hand, for m_X approaching m_Z the electroweak precision bounds on ϵ become stronger (that's why for the benchmark point with $m_X = 60\,\text{GeV}$ we had to choose a slightly smaller value of ϵ). For this reason, in the allowed parameter space, the new physics corrections in the $h \to 4\ell$ channel quickly become unobservable for $m_X \gtrsim 70\,\text{GeV}$. Finally, we estimate the reach in the kinetic mixing parameter: at the most favorable hidden photon mass $m_X \approx 30\,\text{GeV}$ the high-luminosity LHC will be able to exclude ϵ down to 0.007. The bottom line is that the LHC is capable of exploring new interesting regions of the parameter space, even in the simplest version of the hidden photon model.

The next step is to go beyond the simplest hidden photon model and to allow $\epsilon_2 \neq 0$ and or $\epsilon_3 \neq 0$ in eq. (2.9). As explained previously, this extended model allows us to increase new physics corrections to the $h \to 4\ell$ rate, which greatly improves the sensitivity at the LHC. In fact, the strongest constraints on this model are currently provided by the LHC Higgs measurements, in particular for $m_X = 30\,\text{GeV}$ we find $\epsilon_2 \lesssim 0.015$, $\epsilon_3 \lesssim 0.02$. In the left panel of figure 5 we show the results for a couple of scenarios with $m_X = 30\,\text{GeV}$.

[4]Assuming that the cut on the lepton pair invariant mass can be lowered from the current standard value of 12 GeV.

JHEP12(2014)037

Our benchmark points are chosen such that the $h \to 4\ell$ rate is significantly enhanced, by 20–30%, which is not far from the current upper limit. For this reason the rate information alone should be enough to exclude these scenarios at the LHC run-II. Taking advantage of the shape information further improves the sensitivity. We find that also in this case the shape information has a much stronger discriminating power, as can be clearly seen in the right panel of figure 5. Combining the two, the LHC experiments should be able to comfortably exclude[5] our two benchmarks already after the first year of the coming LHC run.

We note that the discriminating power is increased thanks to the $hX\gamma$ couplings present in the extended model, see eq. (2.11). This is partly due to the fact the diagrams with an off-shell photon increase the new physics contribution to the $h \to 4\ell$ rate. But on top off that the the photon contributions lead to larger shape differences with respect to the SM, primarily in the invariant mass distributions. See [23] for a study of this effect in a different context. Another consequence of the $hX\gamma$ coupling is that the LHC is sensitive to larger values of m_X which would be kinematically suppressed if only hZX couplings were present. This allows the golden channel to probe a larger range of hidden photon masses than might be naively expected, even up to $m_X \sim 100\,\text{GeV}$. Finally, we point out that the golden channel is sensitive not only to the magnitude but also to the signs of ϵ_2 and ϵ_3 relative to that of ϵ. Indeed, we find that for the parameter space regions where there is sensitivity to exotic Higgs decays we can discriminate between the positive and negative ϵ_2 or ϵ_3 hypotheses.

Throughout our analysis we used the full information about the shape of the differential distribution in the M_1, M_2, and angular variables. However, the sensitivity is clearly dominated by the occurrence of a resonance for M_2 equal to the hidden photon mass. It is interesting to ask the question whether the full shape analysis is any way superior to a simple bump-hunting in the M_2 variable that was pursued in refs. [15, 16, 30, 43]. We compared the performance of the different methods for our benchmark points with $m_X = 30\,\text{GeV}$. We first compared the M_2 bump-hunting procedure to a simplified version of matrix element method using only M_1 and M_2 as discriminating variables. For the vanilla hidden-photon scenario, we find the latter method improves the sensitivity by about 10%. In this case the full shape analysis does not lead to any further noticeable improvements, which is understandable given the tensor structure of the hidden photon coupling to the Higgs boson is the same as in the SM. For the extended scenario with non-zero ϵ_2 or ϵ_3 the improvement over the bump-hunting method is more prominent. Using only M_1 and M_2, we find that the sensitivity is roughly 20% better than for M_2 bump-hunting. The better performance can be traced to the coupling of the Higgs to 1 hidden and 1 ordinary photon present in this model, which significantly affects the shape of M_2 at the low end of the spectrum. For the extended model, we find that the full shape analysis leads to another 5% improvement, taking advantage of the fact that the tensor structure of the hidden photon coupling to the Higgs boson differs from the one in the SM.

The final exotic Higgs scenario we study here is the vector-like lepton mixing with the SM muon. The benchmarks points we analyzed are summarized in table 1, and the

[5] Or to discover.

JHEP12(2014)037

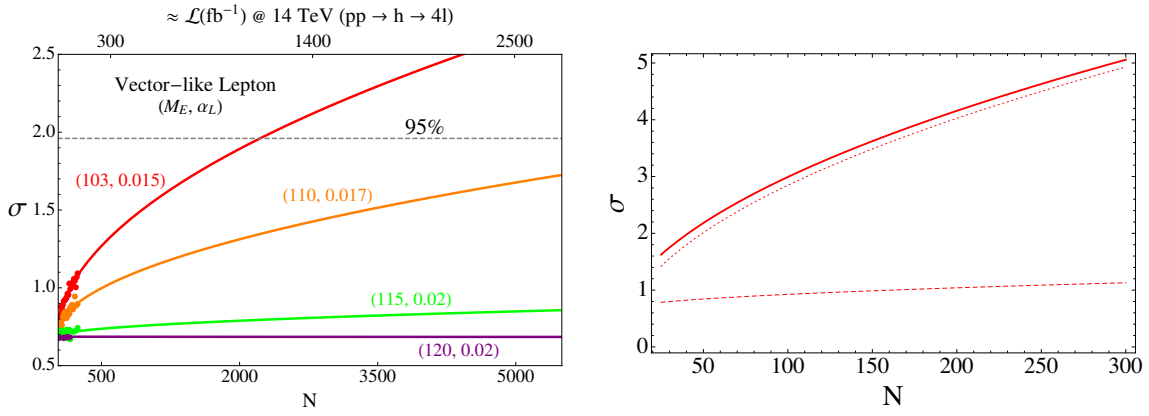

Figure 6. *Left*: lHC sensitivity using the shape of the 4-lepton distribution alone for the vector-like lepton points labeled by the values of (M_E, α_L). The dots indicate the results obtained by conducting pseudo-experiments which are then extrapolated to larger N assuming the significance grows as $\sqrt{N}$. *Right*: comparison of the discrimination power using the shape (dashed), rate (dotted), and combined shape+rate information (solid) for the benchmark point with $M_E = 103\,\text{GeV}$, $\alpha_L = 0.015$.

results are shown in figure 6. We see that the sensitivity quickly decreases as the vector-like lepton mass M_E approaches the Higgs boson mass. One reason is that $\text{Br}(h \to E\mu)$ gets kinematically suppressed for $M_E \approx m_h$. On top of that, the muon emitted in the $h \to E\mu$ decay is very soft, therefore it often does not pass experimental cuts. Thus, there is a rather small window above the LEP limit $M_E \approx 103\,\text{GeV}$ where the LHC is able to probe this model.

We find that in this model the LHC sensitivity is much weaker than in the hidden photon case if only the shape observables are used, see the left panel of figure 6. This is because the differential distributions in this model lack a prominent feature, such as the resonance in M_2 in the hidden photon model. Although, the model predicts a peak in the $m_{3\ell}$ distributions at $m_{3\ell} = M_E$, we find it provides much less discriminating power. That peak does not stand out prominently on top of the SM background, as the $m_{3\ell}$ distribution in the SM is also peaked around 100 GeV (since the $m_{2\ell}$ distribution peaks near the Z boson mass, and $m_{4\ell} = 125\,\text{GeV}$). We find that the differential spectrum in the vector-like lepton model with M_E in the interesting range is in fact quite similar to the SM one. That fact together with the combinatorial background make the shape analysis less efficient in this model. Discriminating the model using shape observables and standard CMS cuts is possible only when large statistics is accumulated, and only in the narrow mass window $103\,\text{GeV} \leq m_E \lesssim 115\,\text{GeV}$. On the other hand, the total event rate is in this case a much stronger discriminator, as shown in the right panel of figure 6. Thus, by simply counting the number of events in the $2e2\mu$ and 4μ channels, we can explore new regions of the M_E-α_L parameter space for $103\,\text{GeV} \leq m_E \lesssim 115\,\text{GeV}$. In particular, for $m_E = 103\,\text{GeV}$ we estimate the LHC experiments can probe α_L down to ~ 0.007. Observing an excess of 4μ and $2e2\mu$ events would be a motivation to apply model-specific cuts, to isolate the vector-like lepton signal. Similar comments apply to a vector-like lepton

JHEP12(2014)037

mixing with the SM electron, except that then an excess is expected in the $4e$ and $2e2\mu$ channels. Finally, we note E could mix predominantly with the τ lepton, which is in fact the most natural possibility from the point of view of models where vector-like leptons play a role in generating the SM fermion mass hierarchies. Thus, exploring also the $2\ell 2\tau$ final state would be advantageous in this context.

5 Summary

In this paper we studied the prospects of constraining exotic Higgs decays using the 4-lepton final state. We picked two scenarios of more general interest: a hidden photon mixing with the SM via the hypercharge portal, and a vector-like charged lepton mixing with one of the SM leptons via Yukawa interactions. Using the rate information only, the LHC run-II is sensitive to exotic decays if the new contributions to the total $h \to 4\ell$ rate are larger than 10% of the SM rate. This is possible to arrange in the vector-like lepton scenario, and also in the non-minimal hidden photon scenario in the presence of direct Higgs interactions with the hidden sector. The main point of this paper is to argue that taking advantage of the full information contained in the differential distribution of the 4-lepton final state dramatically improves the LHC sensitivity. To extract that information, we employed the matrix element methods previously developed in the context of measuring the coupling strength and the tensor structure of Higgs interactions with the SM gauge fields. These methods can be carried over to our case in a straightforward way, as exotic Higgs decays may readily affect the shape of the 4-lepton differential distribution. The shape information is essential in constraining the minimal version of the hidden photon model, where corrections to the total $h \to 4\ell$ are not expected to exceed a few percent. We find that for the hidden photon masses between 15 and 65 GeV the run-II of the LHC will be able to probe a new parameter space of the hidden photon model that is currently allowed by all precision constraints. Likewise, in the non-minimal hidden photon scenario, the shape information allows one to significantly improve the sensitivity such that large chunks of the allowed parameter space can be explored already in the first year of the upcoming LHC run.

Acknowledgments

We thank Yi Chen and Kunal Kumar for the help with simulations and validation as well as Jessie Shelton for interesting discussions. We also thank Centro de Ciencias de Benasque Pedro Pascual for their hospitality during which much of this work was completed. This work was supported by the ERC advanced grant Higgs@LHC.

JHEP12(2014)037

References

[1] ATLAS collaboration, *Observation of a new particle in the search for the standard model Higgs boson with the ATLAS detector at the LHC*, *Phys. Lett.* **B 716** (2012) 1 [arXiv:1207.7214] [INSPIRE].

[2] CMS collaboration, *Observation of a new boson at a mass of 125 GeV with the CMS experiment at the LHC*, *Phys. Lett.* **B 716** (2012) 30 [arXiv:1207.7235] [INSPIRE].

[3] CMS collaboration, *Search for invisible decays of Higgs bosons in the vector boson fusion and associated ZH production modes*, *Eur. Phys. J.* **C 74** (2014) 2980 [arXiv:1404.1344] [INSPIRE].

[4] ATLAS collaboration, *Search for invisible decays of a Higgs boson produced in association with a Z boson in ATLAS*, *Phys. Rev. Lett.* **112** (2014) 201802 [arXiv:1402.3244] [INSPIRE].

[5] ATLAS collaboration, *Search for a Higgs boson decaying to four photons through light CP-odd scalar coupling using 4.9 fb^{-1} of 7 TeV pp collision data taken with ATLAS detector at the LHC*, ATLAS-CONF-2012-079 (2012).

[6] CMS collaboration, *Search for a non-standard-model Higgs boson decaying to a pair of new light bosons in four-muon final states*, CMS-PAS-HIG-13-010 (2013).

[7] ATLAS collaboration, *Search for displaced muonic lepton jets from light Higgs boson decay in proton-proton collisions at $\sqrt{s} = 7$ TeV with the ATLAS detector*, *Phys. Lett.* **B 721** (2013) 32 [arXiv:1210.0435] [INSPIRE].

[8] ATLAS collaboration, *Search for WH production with a light Higgs boson decaying to prompt electron-jets in proton-proton collisions at $\sqrt{s} = 7$ TeV with the ATLAS detector*, *New J. Phys.* **15** (2013) 043009 [arXiv:1302.4403] [INSPIRE].

[9] ATLAS collaboration, *Search for a light Higgs boson decaying to long-lived weakly-interacting particles in proton-proton collisions at $\sqrt{s} = 7$ TeV with the ATLAS detector*, *Phys. Rev. Lett.* **108** (2012) 251801 [arXiv:1203.1303] [INSPIRE].

[10] CMS collaboration, *Search in the displaced lepton channel for heavy resonances decaying to long-lived neutral particles*, CMS-PAS-EXO-11-101 (2012).

[11] G. Blankenburg, J. Ellis and G. Isidori, *Flavour-changing decays of a 125 GeV Higgs-like particle*, *Phys. Lett.* **B 712** (2012) 386 [arXiv:1202.5704] [INSPIRE].

[12] R. Harnik, J. Kopp and J. Zupan, *Flavor violating Higgs decays*, *JHEP* **03** (2013) 026 [arXiv:1209.1397] [INSPIRE].

[13] G. Isidori, A.V. Manohar and M. Trott, *Probing the nature of the Higgs-like boson via $h \to V\mathcal{F}$ decays*, *Phys. Lett.* **B 728** (2014) 131 [arXiv:1305.0663] [INSPIRE].

[14] J. Huang, T. Liu, L.-T. Wang and F. Yu, *Supersymmetric exotic decays of the 125 GeV Higgs boson*, *Phys. Rev. Lett.* **112** (2014) 221803 [arXiv:1309.6633] [INSPIRE].

[15] M. Gonzalez-Alonso and G. Isidori, *The $h \to 4\ell$ spectrum at low m_{34}: standard model vs. light new physics*, *Phys. Lett.* **B 733** (2014) 359 [arXiv:1403.2648] [INSPIRE].

[16] D. Curtin et al., *Exotic decays of the 125 GeV Higgs boson*, *Phys. Rev.* **D 90** (2014) 075004 [arXiv:1312.4992] [INSPIRE].

[17] ATLAS collaboration, *Measurements of the properties of the Higgs-like boson in the four lepton decay channel with the ATLAS detector using 25 fb^{-1} of proton-proton collision data*, ATLAS-CONF-2013-013 (2013).

JHEP12(2014)037

[18] CMS collaboration, *Measurement of the properties of a Higgs boson in the four-lepton final state*, *Phys. Rev.* **D 89** (2014) 092007 [arXiv:1312.5353] [INSPIRE].

[19] LHC Higgs Cross Section Working Group, S. Heinemeyer et al., *Handbook of LHC Higgs cross sections: 3. Higgs properties*, arXiv:1307.1347 [INSPIRE].

[20] CMS collaboration, *Constraints on the Higgs boson width from off-shell production and decay to $ZZ \to \ell\ell\ell'\ell'$ and $\ell\ell\nu\nu$*, CMS-PAS-HIG-14-002 (2014).

[21] Y. Chen and R. Vega-Morales, *Extracting effective Higgs couplings in the golden channel*, *JHEP* **04** (2014) 057 [arXiv:1310.2893] [INSPIRE].

[22] Y. Chen et al., *8D likelihood effective Higgs couplings extraction framework in the golden channel*, arXiv:1401.2077 [INSPIRE].

[23] Y. Chen, R. Harnik and R. Vega-Morales, *Probing the Higgs couplings to photons in $h \to 4\ell$ at the LHC*, *Phys. Rev. Lett.* **113** (2014) 191801 [arXiv:1404.1336] [INSPIRE].

[24] B. Holdom, *Two* U(1)*'s and ϵ charge shifts*, *Phys. Lett.* **B 166** (1986) 196 [INSPIRE].

[25] ALEPH, DELPHI, L3, OPAL, SLD, LEP Electroweak Working Group, SLD Electroweak Group and SLD Heavy Flavour Group collaborations, S. Schael et al., *Precision electroweak measurements on the Z resonance*, *Phys. Rept.* **427** (2006) 257 [hep-ex/0509008] [INSPIRE].

[26] Tevatron Electroweak Working Group, *2012 update of the combination of CDF and D0 results for the mass of the W boson*, arXiv:1204.0042 [INSPIRE].

[27] A. Hook, E. Izaguirre and J.G. Wacker, *Model independent bounds on kinetic mixing*, *Adv. High Energy Phys.* **2011** (2011) 859762 [arXiv:1006.0973] [INSPIRE].

[28] J.D. Bjorken, R. Essig, P. Schuster and N. Toro, *New fixed-target experiments to search for dark gauge forces*, *Phys. Rev.* **D 80** (2009) 075018 [arXiv:0906.0580] [INSPIRE].

[29] BaBar collaboration, B. Aubert et al., *Search for dimuon decays of a light scalar boson in radiative transitions $\Upsilon \to \gamma A^0$*, *Phys. Rev. Lett.* **103** (2009) 081803 [arXiv:0905.4539] [INSPIRE].

[30] S. Gopalakrishna, S. Jung and J.D. Wells, *Higgs boson decays to four fermions through an abelian hidden sector*, *Phys. Rev.* **D 78** (2008) 055002 [arXiv:0801.3456] [INSPIRE].

[31] H. Davoudiasl, H.-S. Lee, I. Lewis and W.J. Marciano, *Higgs decays as a window into the dark sector*, *Phys. Rev.* **D 88** (2013) 015022 [arXiv:1304.4935] [INSPIRE].

[32] Particle Data Group, J. Beringer et al., *Review of particle physics*, *Phys. Rev.* **D 86** (2012) 010001 [INSPIRE].

[33] CMS collaboration, *A search for anomalous production of events with three or more leptons using 19.5/fb of $\sqrt{s} = 8$ TeV LHC data*, CMS-PAS-SUS-13-002 (2013).

[34] A. Falkowski, D.M. Straub and A. Vicente, *Vector-like leptons: Higgs decays and collider phenomenology*, *JHEP* **05** (2014) 092 [arXiv:1312.5329] [INSPIRE].

[35] D. Stolarski and R. Vega-Morales, *Directly measuring the tensor structure of the scalar coupling to gauge bosons*, *Phys. Rev.* **D 86** (2012) 117504 [arXiv:1208.4840] [INSPIRE].

[36] Y. Gao et al., *Spin determination of single-produced resonances at hadron colliders*, *Phys. Rev.* **D 81** (2010) 075022 [arXiv:1001.3396] [INSPIRE].

JHEP12(2014)037

[37] A. De Rujula, J. Lykken, M. Pierini, C. Rogan and M. Spiropulu, *Higgs look-alikes at the LHC*, *Phys. Rev.* **D 82** (2010) 013003 [arXiv:1001.5300] [INSPIRE].

[38] Y. Chen, N. Tran and R. Vega-Morales, *Scrutinizing the Higgs signal and background in the $2e2\mu$ golden channel*, *JHEP* **01** (2013) 182 [arXiv:1211.1959] [INSPIRE].

[39] T. Hahn, *Generating Feynman diagrams and amplitudes with FeynArts 3*, *Comput. Phys. Commun.* **140** (2001) 418 [hep-ph/0012260] [INSPIRE].

[40] N.D. Christensen and C. Duhr, *FeynRules — Feynman rules made easy*, *Comput. Phys. Commun.* **180** (2009) 1614 [arXiv:0806.4194] [INSPIRE].

[41] R. Cousins, J. Mumford, J. Tucker and V. Valuev, *Spin discrimination of new heavy resonances at the LHC*, *JHEP* **11** (2005) 046 [INSPIRE].

[42] J. Alwall, M. Herquet, F. Maltoni, O. Mattelaer and T. Stelzer, *MadGraph 5: going beyond*, *JHEP* **06** (2011) 128 [arXiv:1106.0522] [INSPIRE].

[43] H. Davoudiasl, H.-S. Lee and W.J. Marciano, *"Dark" Z implications for parity violation, rare meson decays, and Higgs physics*, *Phys. Rev.* **D 85** (2012) 115019 [arXiv:1203.2947] [INSPIRE].

JHEP12(2014)037